UNVEILING THE POTENTIAL OF ADVANCED MODELS FOR MAIN ENGINE POWER OF RO-PAX FERRIES WITH NEURAL NETWORKS AND FUZZY LOGIC

Mitra Vesović, University of Belgrade, mvesovic@mas.bg.ac.rs
Luka Mijatović, University of Belgrade, mijatovic.s.luka@gmail.com

ABSTRACT

This paper discusses the application of artificial intelligence (AI) techniques in the field of marine engineering and naval architecture and explores the potential of AI models in predicting the main engine power of eco-friendly ferries over 5 parameters: length between perpendiculars, beam, draft, deadweight and speed. The research compares neural network and ANFIS against classical linear model providing exact equations of dependency between input and output parameters. The study utilizes an originally formed database consisting of more than 200 Ro-Pax ferries primarily focused on the ones operating in the Mediterranean Sea basin. For the formed database the Energy Efficiency Existing Index (EEXI) calculation is done and ferries complying with the IMO regulation are used for further power prediction. The data collection and analysis process involve preprocessing, outlier detection and statistical comparisons between the AI models and traditional method.

KEYWORDS

Keywords: artificial neural network and fuzzy logic, metaheuristics and prediction, Ro-Pax ferries, energy efficiency

1. INTRODUCTION

In today's rapidly changing world, Artificial Intelligence (AI) has emerged as a significant and essential technology. Its ability to quickly and effectively solve complex problems has made it a crucial tool in various professional fields, such as for example finding mathematical representation of calm-water resistance for contemporary planning hull forms (Radojčić et al.,2014; Radojčić et al., 2019). Artificial intelligence (AI) tools are gaining popularity in marine engineering, although their use has been limited due to the *black box* nature and unclear processes. As global warming challenges the shipping industry to meet environmental requirements, integrating AI can be used as a tool to improve operational efficiency and help ships comply with new environmental regulations. Recent years have seen significant interest and progress in marine vessel performance. Factors like fuel, propulsion, loading, sea conditions, and currents influence ship performance, spurring research on optimization. (Bayraktar 2023). This study undertakes an extensive analysis of data from more than 200 Ro-Pax ferries. By carefully examining data, the research investigates Artificial Neural Networks (ANN) and Fuzzy Inference Systems (FIS) models, utilizing five input parameters: length between perpendiculars (Lpp), beam (B), draft (T), deadweight (DWT) and speed (V). The study not only demonstrates the performance of these models but also provides evidence that employing various AI techniques enables the swift and accurate attainment of the desired outcome – the power of the main engine. The comprehensive analysis includes forming the original database, pre-processing, rejecting unnecessary data (diagnosing outliers) and providing the exact formula for each model. Finally, the aforementioned artificial intelligence models are compared with classical method: Multiple Linear Regression (MLR).

2. REGRESSION MODELS

The primary benefit of employing an ANN model lies in its inherent capacity for self-learning and its ability to effectively capture and approximate complex nonlinear relationships between input variables and output outcomes (Jovanović, 2015). One of the primary factors influencing ship emissions is the power of the main engine (Lee, 2021). Consequently, numerous studies in existing literature have concentrated on determining the optimal main engine power for ships. Lee et al. (Lee, 2021) proposed a deep feed-forward neural network (DFN) that involves data pattern recognition to predict ship power. Similarly, Parkes and others (Parkes, 2018) investigate the use of neural networks to improve the accuracy and flexibility of predicting ship power in different weather conditions. The main idea of many other studies, such as the one provided by Öztürk et al. (Öztürk 2022) is to reduce air pollution and operational costs in shipping through the implementation of efficiency measures using decision support systems based on MLR and ANN, which provide satisfactory fuel oil consumption prediction models, potentially resulting in energy savings. In recent research Ozsari (Ozsari 2023) implements multiple ANN models for the prediction of container, cargo, and tanker ships primary engine power and pollutant emissions.

2.1 FEEDFORWARD BACKPROPAGATION NEURAL NETWORK

In this study, a common ANN architecture, the feedforward neural network (FFNN), was used to predict eco-friendly ferry main engine power. FFNN consists of input, output, and hidden layers with interconnected neurons and adaptable weighted connections. Nonlinear activation functions in the hidden layer enable universal approximation capabilities. To train the artificial neural network, the widely used back-propagation algorithm is typically employed, with various weight and bias adjustment methods like Levenberg-Marquardt, Bayesian regularization, resilient and gradient descent, among others.

2.2 FUZZY-NEURAL MODELS

Fuzzy systems are computational models that use linguistic rules and a rule base to process crisp input data from a database, allowing for flexible handling of uncertainty and imprecision in decision-making. In these systems, decisions are made by applying rules to input data, generating output values representing degrees of membership in fuzzy sets. By combining the benefits of training possessed by neural networks with decision-making similar to human methodology, synergy is achieved between ANN and FIS.

2.2 (a) ANFIS

ANFIS was first developed by Jang, (Jang 1993). The structure of ANFIS is made up of five layers, and it is usual that papers show a structure with two inputs x_k, k = 1,2 and one output, Figure 1, based on the first-order Takagi–Sugeno model, with the two membership functions (MF) j = 1,2 and four rules m = 1,2…4. A typical set of rules can then be written as:

$$\textbf{If } x_1 \textbf{ is } A_{11} \textbf{ and } x_2 \textbf{ is } A_{12} \textbf{ then } f_1 = q_{11}x_1+q_{12}x_2+c_1$$

$$\textbf{If } x_1 \textbf{ is } A_{11} \textbf{ and } x_2 \textbf{ is } A_{22} \textbf{ then } f_2 = q_{21}x_1+q_{22}x_2+c_2,$$

$$\textbf{If } x_1 \textbf{ is } A_{21} \textbf{ and } x_2 \textbf{ is } A_{12} \textbf{ then } f_3 = q_{31}x_1+q_{32}x_2+c_3$$

$$\textbf{If } x_1 \textbf{ is } A_{21} \textbf{ and } x_2 \textbf{ is } A_{22} \textbf{ then } f_4 = q_{41}x_1+q_{42}x_2+c_4,$$

where A_{1k}, $A_{2k,\ldots,}A_{jk}$ are linguistic labels, q_{mk} and c_m are the consequent parameters. The output of each rule is a linear combination of input variables.

In the first layer of the ANFIS model, the membership degree $\mu_{A_{ik}}$ of *k-th* input is calculated and then passed to the second layer.

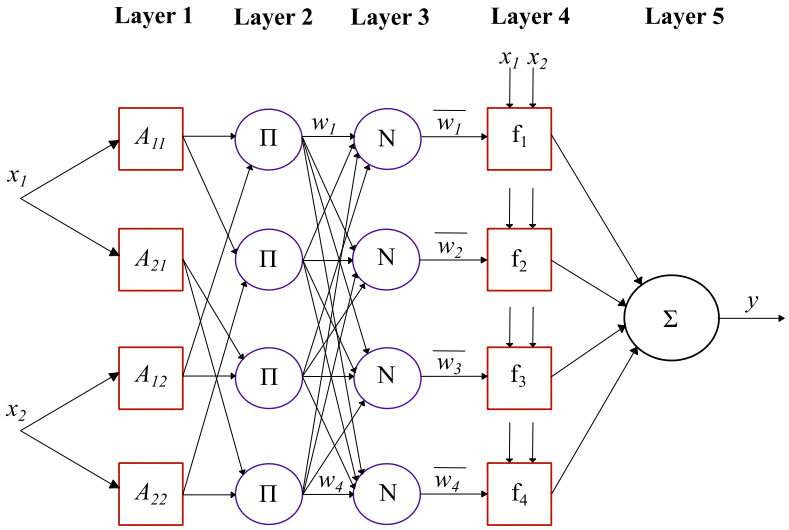

Figure 1: ANFIS architecture with two inputs

An example of a Gaussian membership function, which is characterized by two parameters, standard deviation β and mean α or premise parameters, Eq. (1).

$$\mu_{A_{ik}}(x_k) = e^{-\frac{(x_k-\alpha_{ik})^2}{2\beta_{ik}^2}}. \quad (1)$$

The second layer of the ANFIS model differs from the previous layer in that the nodes in this layer remain fixed. The output of each node in the second layer represents the firing strength w_m of the corresponding rule. It is obtained using T-norm * between two membership degrees.

$$\begin{aligned} w_1 &= \mu_{A_{11}}(x_1) * \mu_{A_{12}}(x_2), \\ w_2 &= \mu_{A_{11}}(x_1) * \mu_{A_{22}}(x_2), \\ w_3 &= \mu_{A_{21}}(x_1) * \mu_{A_{12}}(x_2), \\ w_4 &= \mu_{A_{21}}(x_1) * \mu_{A_{22}}(x_2). \end{aligned} \quad (2)$$

The third layer of ANFIS model performs the computation of the normalized firing strength for each rule. This is achieved by dividing the firing strength of a rule by the sum of all firing strengths.

$$\overline{w}_m = \frac{w_m}{\sum_m w_m}, \quad (3)$$

where m = 1,2…4. In the fourth layer of the ANFIS model, the product of the normalized firing strength and the consequent parameters (q_m and c_m) of each rule is calculated.

$$\overline{w}_m f_m = \overline{w}_m \sum_{k=1}^{2} q_{mk} + c_m. \quad (4)$$

The fifth and final layer of the ANFIS model aggregates the weighted consequent values obtained from all rules.

$$\mathrm{y} = \sum_{m=1}^{4} \overline{w}_m f_m = \frac{1}{\sum_{m=1}^{4} w_m} \sum_{m=1}^{4} w_m \left(\sum_{k=1}^{2} q_{mk} + c_m\right). \quad (5)$$

3. TRADITIONAL REGRESSION MODELS

Traditional models like multiple linear regression rely on explicit mathematical equations. Although newer models may offer flexibility, classical models often excel in interpretability, ease of use, clear assumptions, stability, and robustness. They assume a linear relationship between the target and multiple predictors.

4. CASE STUDY

Due to its geographical characteristics, with a coastline stretching over 68,000 km and more than 2,400 inhabited islands, Europe is a heavily trafficked ferry region. The highest concentration of ferry transport is situated in the Baltic, Northern, and Mediterranean Sea regions of Europe, with over 50% of the total number of routes operating in the Mediterranean Sea alone. Figure 2 (left) illustrates the percentage distribution of ferry routes in the mentioned regions over the years.

The originally collected and compiled database primarily refers to ferries commuting in the Mediterranean Sea under the flags of Greece and Italy. During the formation of the base, the basic criteria were that all ships are classified as Passenger/Ro-Ro Ship (Ro-Pax), that they must be under classification society at the time, that the flag corresponds to the two mentioned countries above and that the gross tonnage (GT) is bigger than 400, so the EEXI rules are applicable.

The formed database includes 215 ferry ships. The largest number of ships belongs to the Italian classification society RINA (Registro Italiano Navale) with a percentage of 84.7%, followed by the Russian RS (Russian Maritime Register of Shipping) with 4.8%, the French BV (Bureau Veritas) with 3.8%, the English LR (Lloyd's Register) with 3.3%, the Polish PRS (Polish Register of Shipping) with 2.4%, and finally, the American ABS (American Bureau of Shipping) and the Korean KRS (Korean Register of Shipping) with 0.5% each.

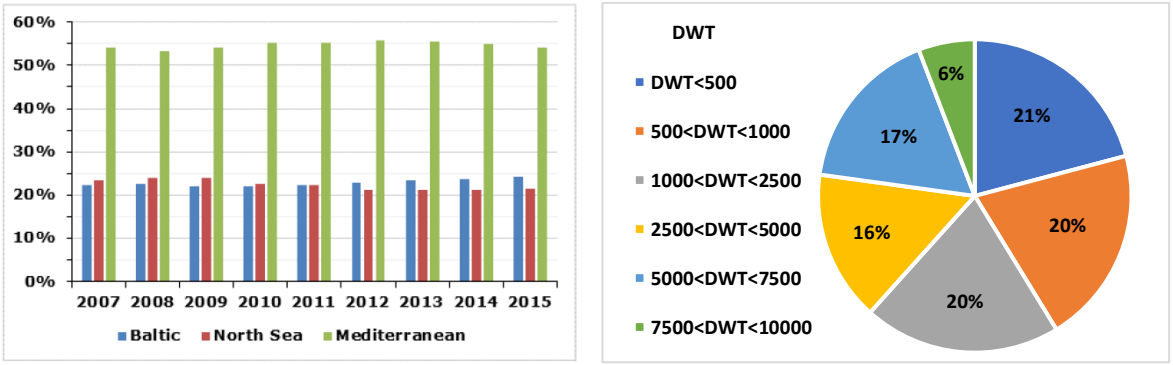

Figure 2: Percentage share of ferry routes in the seas of Europe (https://www.shippax.com/ - left) and DWT distribution of the ferries in database (right).

The average age of ferries in the database is 30 years, 29 for Greek ships and 31 for Italian ones. The most common configurations are with two engines (109 ships) and four engines (85 ships), while the smallest number of ships has six engines (2 ships). Figure 2 (right) shows the distribution of ships in the database according to deadweight tonnage, which ranges from 500 to 10000. This can be explained by the large number of different routes on which ferries operate. Different routes require different capacity needs, some requiring higher passenger capacity and lower vehicle capacity, and vice versa, hence the heterogeneous distribution of DWT.

In Figure 3 (left), the number of ferries is shown as a function of the length between perpendiculars, with the ships grouped in intervals of ten meters. Figure 3 depicts the number of ferries depending on the beam (right) grouped in intervals of two meters. Figure 4 depict the number of ferries depending on draft (left) and speed (right). The ships are grouped in intervals of 0.5 meters for draft in range from 1.47 m to 8.35 m. The speeds of the ships in the database are ranging from 8.4 knots to 42 knots, when calculated to Froude number from 0.2 to 0.85, with an average speed of 21.4 knots, which is typical for this type of vessel as they are among the fastest cargo ships.

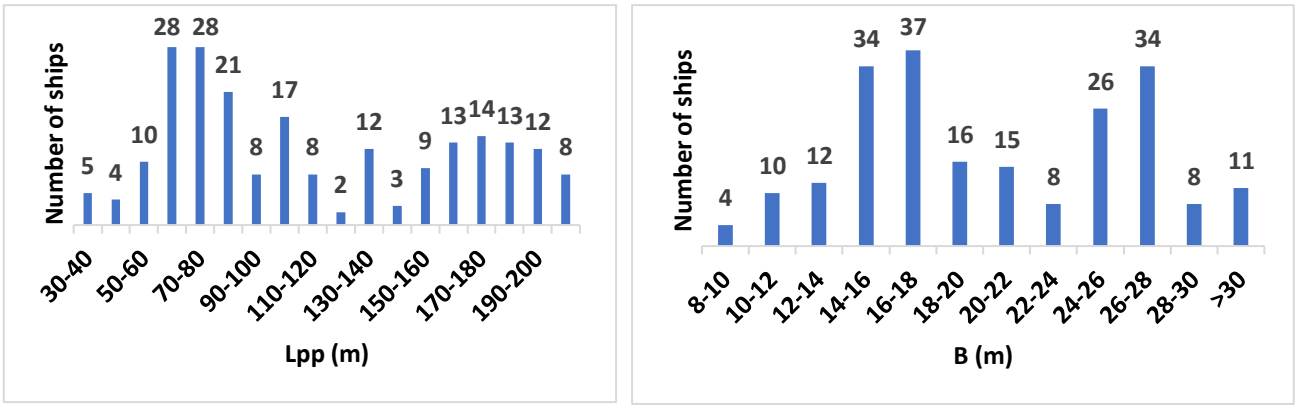

Figure 3: Number of ferries shown as a function of the length between perpendicular (left) and beam (right)

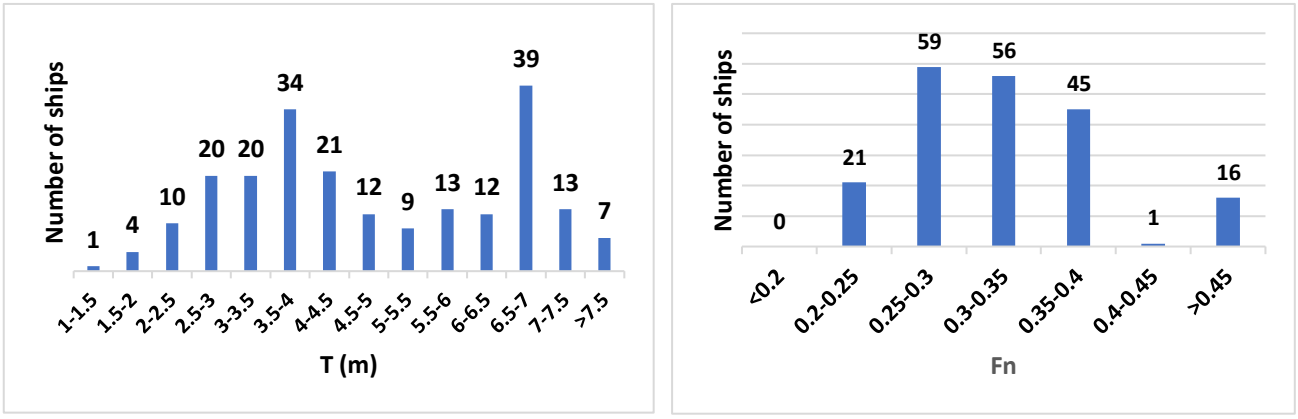

Figure 4: Number of ferries shown as a function of the draft (left) and speed given in Froud number (right)

4.1 DATA PRE-PROCESSING

IMO is actively trying to reduce greenhouse gas emissions from shipping. One of the measures to achieve this was newly introduced EEXI requirement to improve energy efficiency of existing ships, which also include Ro-Pax ferries. The EEXI is a numerical value based on technical characteristics of the vessel like engine power, size and design characteristics. Though complying with EEXI is challenging, it encourages innovation and adoption of advanced technologies in maritime sector to comply with newly introduced IMO regulations leading to more environmentally friendly fleet of Ro-Pax ferries.

For each ferry ship in the database an attained EEXI and a required EEXI values are calculated, according to procedure given in MEPC.333(76). In order that the ship could be considered as energy efficient, attained EEXI should be lower than a required EEXI: Attained *EEXI* ≤ Required *EEXI*. Attained EEXI is calculated as per simplified formula Eq. (6).

$$\text{Attained } EEXI = \frac{P_{ME} \cdot C_{FME} \cdot SFC_{ME} + P_{AE} \cdot C_{FAE} \cdot SFC_{AE}}{f_i \cdot f_c \cdot f_l \cdot Capacity \cdot f_w \cdot V_{ref} \cdot f_m} \quad (6)$$

The numerator in the EEXI formula generally represents CO_2 mass flow produced based on the ship systems power needs, and the denominator represents benefit for the society (transport work). In general, the symbols in Eq. (6) have the following meaning: P_{ME} and P_{AE} are main and auxiliary engine power, C_{FME} and C_{FAE} are conversion factor between fuel consumption and CO_2 emission for main and auxiliary engine, SFC_{ME} and SFC_{AE} are specific fuel oil consumption for main and auxiliary engine, V_{REF} is reference speed and *Capacity* is equal to deadweight of the ship. The f_i, f_c, f_l, f_w, f_m are correction factors which depend on type and design characteristic of the cargo ship. Two correction

factors are specially introduced for Ro-Pax ships. First one is fj_{RoRo} which corrects EEXI values for ships with high Froude number i.e. higher speed and second one is f_{cRoPax} cubic correction factor which partially replaces DWT as a measure of ship capacity with GT. The fallowing factors can be calculated as per Eq. (7) and Eq (8).

$$f_{jRoRo} = \frac{1}{F_n^{\alpha} \cdot \left(\frac{Lpp}{B}\right)^{\beta} \cdot \left(\frac{B}{T}\right)^{\gamma} \cdot \left(\frac{Lpp}{\nabla^{1/3}}\right)^{\delta}}, \quad (7)$$

where: α = 2.50, β = 0.75, γ = 0.75 and δ = 1.00 and ∇ is displacement (volume) coefficient.

$$f_{cRoPax} = \left(\frac{DWT/GT}{0.35}\right)^{-0.8}. \quad (8)$$

Taking the values from MEPC.333(76) for C_{FME}, S_{FCME}, C_{FAE}, S_{FCAE}, correction factors and implementing two Ro-Pax correction factors in Eq. (6) the Attained EEXI is calculated as per Eq. (9).

$$\text{Attained } EEXI = 3.1144 \frac{f_{jRoRo} \cdot 190 \cdot \sum_{i=1}^{nME} P_{ME(i)} + 215 \cdot P_{AE}}{f_{\text{cRoPax}} \cdot \text{Capacity} \cdot V_{\text{ref}}} \quad (9)$$

The required EEXI is calculated as Eq. (10):

$$\text{Required } EEXI = \left(1 - \frac{Y}{100}\right) \cdot \text{Reference line}, \quad (10)$$

where Y is reduction factor given for each type of cargo vessels depending on their size in DWT. Reference line is given with expression: Reference line = $a \cdot b^{-c}$, where coefficient a,b and c are given in the MEPC.328(76) for each type of cargo ships.

After conducting the calculation on the filtered database, it was found that 87% of the ferry boats comply with the IMO regulations, while only 13% do not. The ships that comply with EEXI, along with the percentage breakdown by decades and the percentage breakdown by DWT, are provided in the Figure 5, below (Mijatović 2023). For further calculations in the study, only the ships that satisfy EEXI requirements have been adopted. Before developing further models, certain rules and limitations had to be established due to the significant heterogeneity of the database, which encompasses various types of ferries.

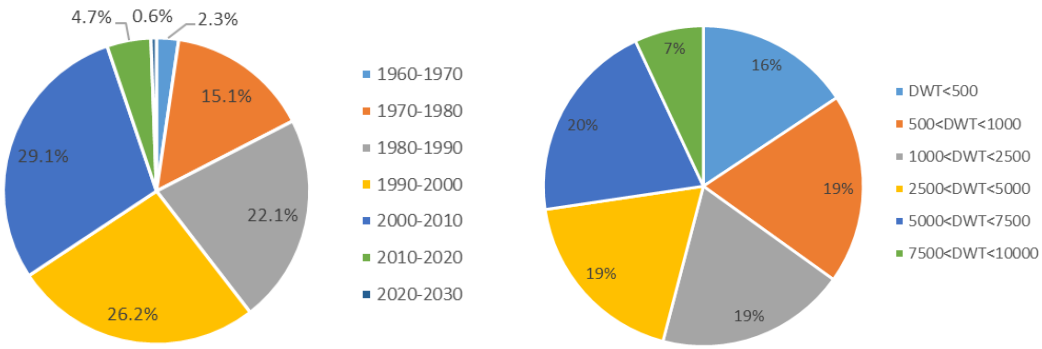

Figure 5: The ships that comply with EEXI

The first step in data filtering was to discard all ships with missing or NaN data for at least one of the following parameters: Lpp, B, V, T, DWT, or P, from further analysis. Atypical elements are objects or entities that, in some sense, have characteristics that differ from the majority of other objects in a data set or have attribute values that are unusual compared to typical values for that attribute.

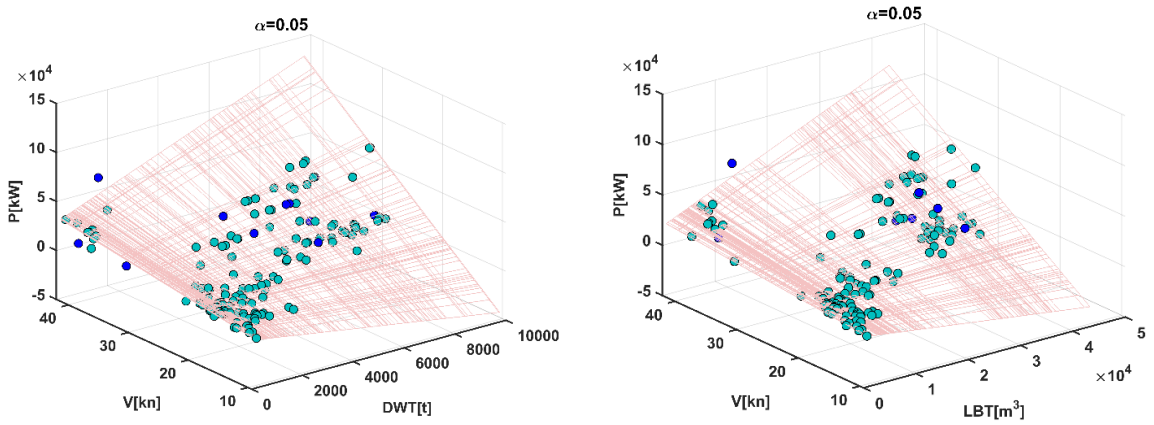

Figure 6: Identification of outlier

To identify outliers within the given dataset, two multiple linear regression models were constructed. The first model examines the relationship between DWT and V as inputs, and P as the output. The second model considers the product of Lpp, B, and T (LBT), along with V, as inputs, and P as the output. The coefficient of determination R^2 and adjusted R^2 for the first are: 0.771 and 0.768, and for the second model: 0.826 and 0.824, respectively. In the context of linear regression and outlier detection, the significance level α plays a role in determining whether a data point is considered an outlier or not. The smaller significance level indicates that higher level of extreme deviation from the expected pattern is required for a data point to be considered an outlier. In this research, α is set to 0.05. LBT-V-P dependence indicates 8 outliers (blue dots on Figure 6 right), but only 2 of them are different from 11 outliers found by DWT-V-P dependence, (Figure 6 left). All of them have been excluded from further analysis.

4.2 SELECTION OF INPUT PARAMETERS AND NORMALIZATION

In this research paper, we employed dimensionless metrics to represent various aspects of the system. Specifically, we used the length beam ratio Lpp/B to describe different configurations and introduced two dimensionless quantities, B/T and slenderness ratio $Lpp/\nabla^{1/3}$, to characterize load ratios.

When forming the base of ferry boats, the most difficult data to obtain was the volumetric displacement (volume) coefficient C_B. In order to be able to calculate the displacement Δ of the other ships in the base, a reference value had to be adopted and it was decided that it should be the mean value of the all collected C_B values. For ships that had volume coefficient values, the displacement was calculated based on them, and for the others it was given as D_{avg}. Precisely for this reason, instead of volume, the displacement of the ship was used in the slenderness ratio. This was done because of the way the ship displacements were obtained for the ferries in the base. It was considered that by introducing the density of sea water, the error made during the estimation of the displacement will further increase and will affect the calculation. In order to overcome this problem, a water density of $1t/m^3$ was adopted, where the values of volume and displacement were equalized.

For shipping companies, the DWT/Δ ratio is an important economic and efficiency factor. It influences a ship's profitability by determining how much cargo can be carried per unit of displacement. Higher ratio typically indicates that a larger portion of the ship's displacement is dedicated to carrying cargo. This ratio is was adopted as the one of the input parameters. As the last parameter, the influence of the sailing speed via the Froude number based on the length was considered: $Fn = V/ (g\ Lpp)^{1/2}$. The output of the mathematical model is a coefficient of delivered power $C_D = 1000\ P/\rho g \nabla V$, which is used for the calculation of the power: x_k= {Lpp/B, B/T, DWT/Δ, $Lpp/\nabla^{1/3}$, Fn} and $y = C_D$.

Before further analysis and model creation, all input and output data must be recalculated to a certain interval. This procedure, known as normalization, is necessary due to scalar independence in linear regression and activation functions in neural networks, i.e. due to the hypersensitivity of those

functions to very small and very large input data values. Normalization is a well-known procedure in all statistical methods and machine learning. In this paper, it is implemented as Eqs. (11)-(12):

$$x_{k,norm} = a + \frac{(x_k - \min(x_k))\,(b-a)}{\max(x_k) - \min(x_k)}, y_{norm} = a + \frac{(y - \min(y))\,(b-a)}{\max(y) - \min(y)}, k = 1,2 \ldots 5,\ 0 < a < b, \quad (11)$$

where: a = 0.05, b = 0.95.
The previous expression can be written more briefly as:

$$x_{k,norm} = p_k x_k + r_k\,, y_{norm} = Ly + G,\ \ k = 1,2 \ldots 5, \quad (12)$$

where: $p_k = \frac{(b-a)}{\max(x_k) - \min(x_k)}$, $r_k = a + \frac{(a-b)\min(x_k)}{\max(x_k) - \min(x_k)}$, $L = \frac{(b-a)}{\max(y) - \min(y)}$, $G = a + \frac{(a-b)\min(y)}{\max(y) - \min(y)}$.

5. FFNN MODEL DEVELOPMENT

The study utilized FFNN models with different architectures, consisting of an input layer, output layer, and one or more hidden layer(s). The activation functions employed were all the sigmoid (sig) for the hidden layer(s) and for the output layer. This function is continuous, differentiable and has the and has a positive range (unlike hyperbolic tangent). The training algorithm employed was the Levenberg–Marquardt (LM). For the FFNN models the number of neurons in the hidden layer was found by a trial-and-error procedure. The optimum structure of the best FFNN models was found to be three hidden layers with 5, 7 and 5 neurons, respectively.
By random selection, the data is divided as follows: 70% of the data is taken for training, 15% for validation, and 15% for testing. Figure 7 shows the comparison of the measured and predicted values for the best FFNN model. The network quality indicator is the correlation number. The diagram in Figure 7 shows how the results are grouped, how much the network outputs deviate for the training (blue line), test (green) and all (red) input data. If the network has learned to fit the data well, the linear fit to this output-target relationship should closely intersect the bottom-left and top-right corners of the plot (dashed lines). Another performance criteria – MAE was also calculated and it can be seen in Table 1. The function constructed from the network is given as Eq. (13):

$$y = \frac{y_{norm}}{\sigma\left(d_1 + \sum_{l=1}^{5}\left(D_{1l}\,\sigma\left(c_l + \sum_{i=1}^{7}\left(C_{li}\,\sigma\left(b_i + \sum_{j=1}^{5}\left(B_{ij}\,\sigma\left(a_j + \sum_{k=1}^{5} A_{jk}\left(\overbrace{p_k x_k + r_k}^{x_{k,norm}}\right)\right)\right)\right)\right)\right)\right)\right) - G}{L}, \quad (13)$$

where x_k is the k^{th} input feature; A_{jk}, B_{ij}, C_{li} and D_{1l} represents weights between corresponding layers, where first index indicates neuron and second indicates input; a_j, b_i, c_l, are biases in hidden and d_1 is bias in output layer. σ is nonlinear activation function. Although activation functions only have to be continuous in parts, in most cases it is suitable to use fully continuous and differentiable functions (on the whole domain). Sigmoidal function is chosen for activation in all layers. $\sigma(x) = \frac{1}{1+e^{-\alpha x}}$, with α set to 1. Other parameters: p_k, r_k, L and G are explained in Normalization (*4.2 Section*).

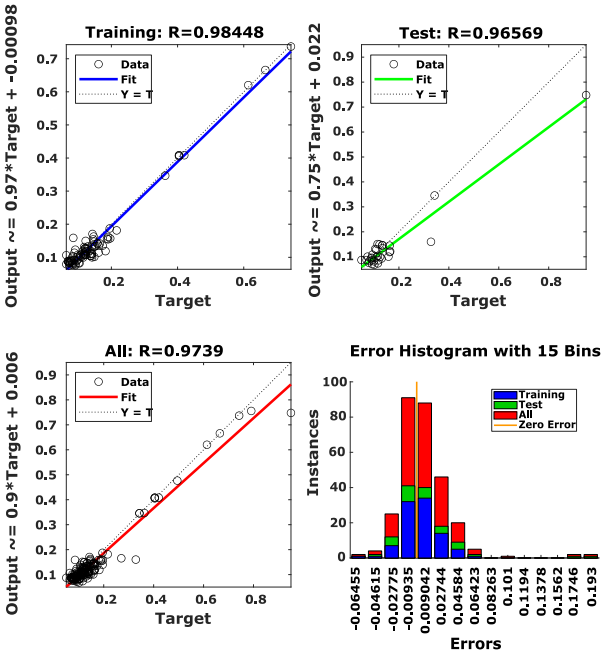

Figure 7: Error and comparison of the measured and predicted values for the best FFNN model

6. ADAPTIVE NEURO-FUZZY INFERENCE SYSTEM

In the present attempt, the number of membership functions assigned to each input variable was chosen empirically by examining the desired input-output data and by trial and error. The initial model, shown on Figure 1, consists of 20 premise parameters, which include 5 inputs and 2 Gaussian membership functions Eq. (1). The algorithm employed to find these parameters is a backpropagation. To extract the initial fuzzy model, the first step involves applying grid partitioning (GP) to the input-output data pairs. The GP method ensures that the membership functions (MFs) are uniformly spaced and have identical shapes. However, this can lead to an exponential increase in the number of rules, even with a moderate number of inputs. In the current scenario, with a fuzzy inference system featuring 5 inputs and only 2 Gaussian membership functions per input, the grid partitioning yields a total of 32 rules (2^5), because of the *curse of dimensionality* (when number of inputs or number of membership functions increases, then the number of fuzzy rules also increases exponentially). In the ANFIS structure presented in this paper, there are a total of 192 consequent parameters, with each of rule having 6 parameters (5 for each input and one independent). Therefore, when considering both the premise and consequent parameters, the overall parameter counts amounts to 212. Of all *T*-norms, product is chosen to be used in the second Layer. Final output from the fuzzy neural network can be calculated using Eq. (14).

$$y = \frac{\overbrace{\frac{1}{\sum_{m=1}^{4} w_m}\sum_{m=1}^{4} w_m\left(\sum_{k=1}^{5} q_{mk}\left(\overbrace{p_k x_k + r_k}^{x_{norm}}\right)+c_m\right)-G}^{y_{norm}}}{L}, \quad (14)$$

where q_{mk} and c_m are consequent parameters (from rules). Although in the terms of training ANFIS model offers promising results, Table 1, this trend does not continue for testing, Figure 8. This could be explained with model complexity, many input arguments and using the grid partitioning which cause the exponential growth of the fuzzy rules and that ANFIS presents a combination of linear polynomial functions in its output. Figure 9 a) – j) shows the dependency of the output on any two inputs. Inputs are taken in the same order as in x_k: input1 = Lpp/B, input2 = B/T, input3 = DWT/Δ, input4 = Lpp/$\nabla^{1/3}$, input5 = Fn and output C_D.

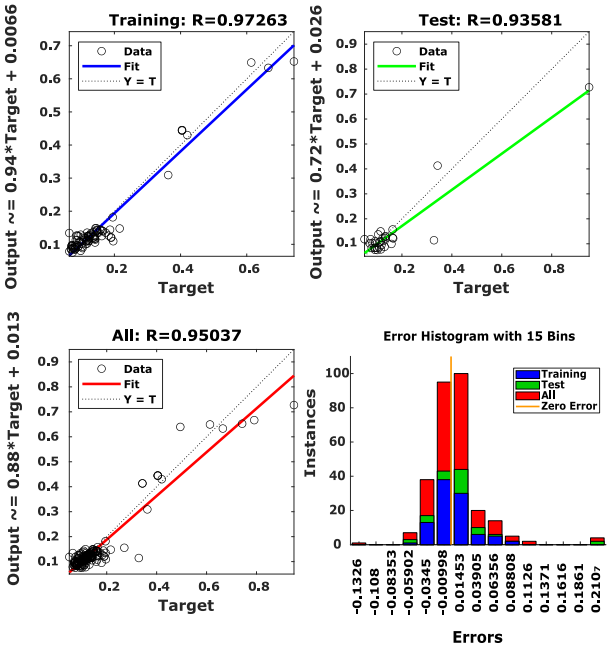

Figure 8: Error and comparison of the measured and predicted values for the best ANFIS model

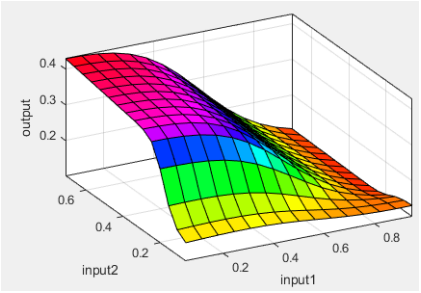

Figure 9: a) Lpp/B, B/T, C_D

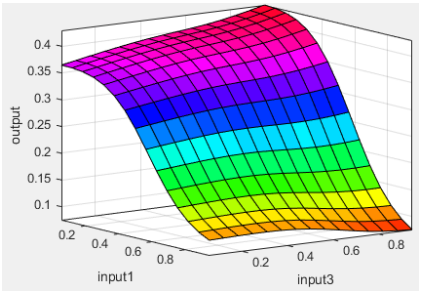

b) Lpp/B, DWT/Δ, C_D

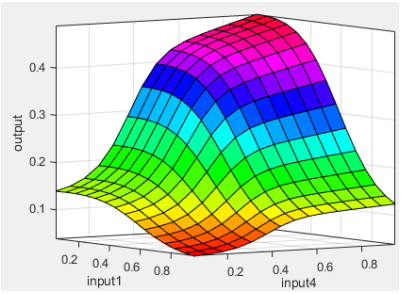

c) Lpp/B, Lpp/$\nabla^{1/3}$, C_D

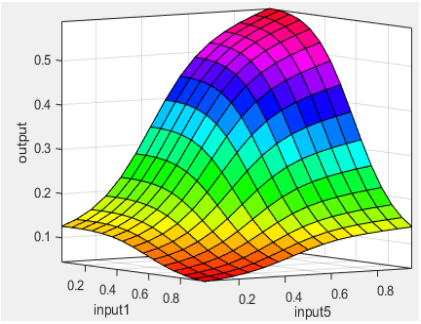

d) Lpp/B, Fn, C_D

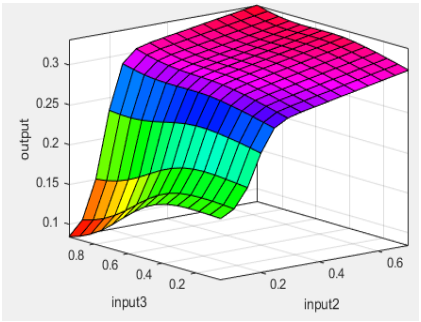

e) B/T, DWT/Δ, C_D

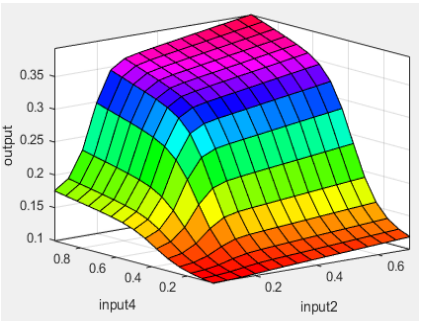

f) B/T, Lpp/$\nabla^{1/3}$, C_D

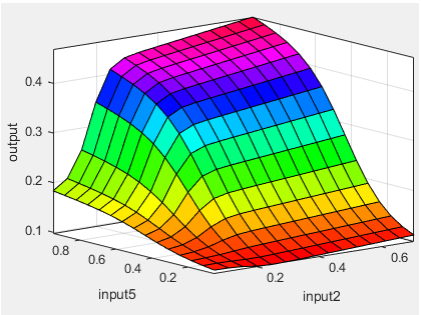

g) B/T, Fn, C_D

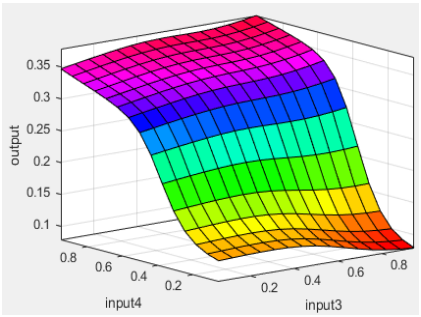

h) DWT/Δ, Lpp/$\nabla^{1/3}$, C_D

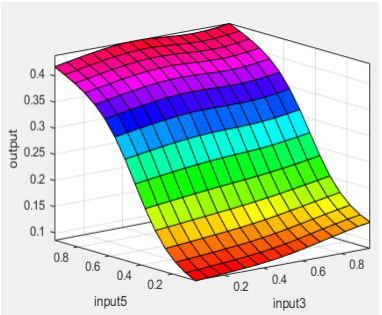

i) DWT/Δ, Fn^3, C_D

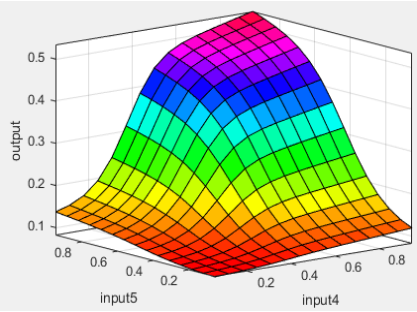

j) $Lpp/\nabla^{1/3}$, Fn, C_D

7. TRADITIONAL MODELS DEVELOPMENT

In this section results from multiple linear regression will be provided. The model, represented by Eq. (15), corresponds to the Multiple Linear Regression approach.

$$y = \frac{\overbrace{\left(\beta_0+\sum_{k=1}^{5}\beta_k\left(\frac{x_{k,norm}}{p_k x_k+r_k}\right)\right)}^{y_{norm}}-G}{L}, \quad (15)$$

where β_0 = 0.1740 and $\boldsymbol{\beta}$ = [-0.7237 -0.2218 0.0461 0.5276 0.4259]. To visually assess the model's performance, Figure 10 illustrates a comparison between the target and predicted values using the MLR model. Notably, the correlation coefficient exceeds 0.94, indicating a strong linear relationship between the predicted and actual values. Because MAE fails to punish large error prediction the best MLR shown the worst results in this criterion, but when it comes to correlation factor measure, ANFIS exhibited the least favourable results

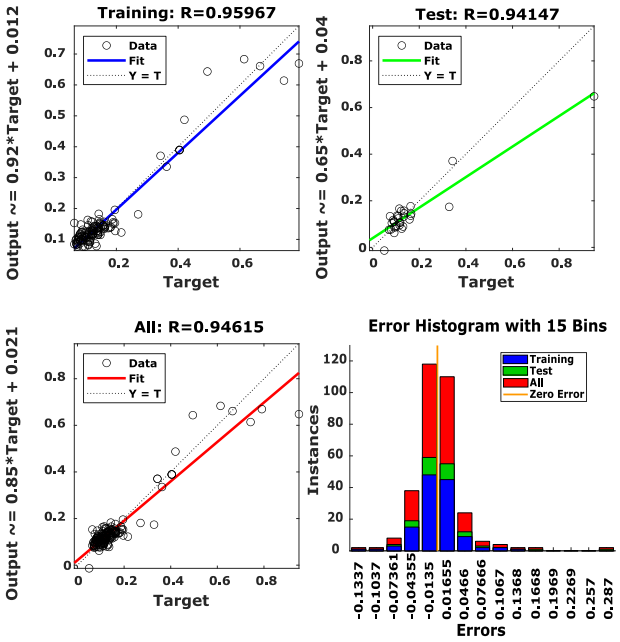

Figure 10: Error and comparison of the measured and predicted values for the best MLR model

Figure 11 presents comparison of all models and the real test data.

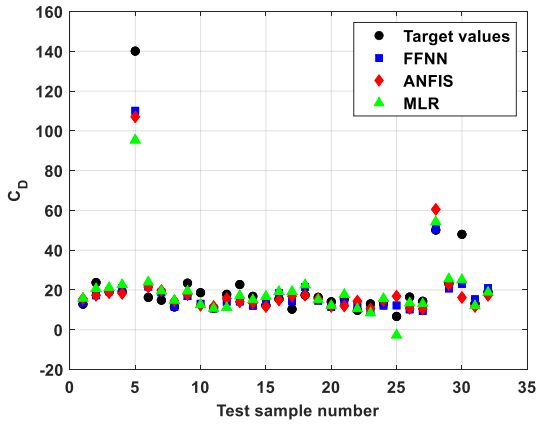

Figure 11: Comparison of the FFNN, ANFIS and MLR

Table 1 summarizes the results obtained by applying the best preformed models for each method in the terms of MAE and R. Parameters of these models are given in Appendix.

Table 1: The best values of MAE and R for modern and traditional regression techniques

Method	Mean absolute error - MAE		Correlation coefficient - R	
	Train dataset	Test dataset	Train dataset	Test dataset
FFNN	**0.01613**	**0.03181**	**0.98448**	**0.96569**
ANFIS	0.02003	0.03638	0.97263	0.93581
MLR	0.02438	0.03696	0.95967	0.94147

In Table 2 the results are averaged over ten independent runs, and the best results are indicated in the bold type.

Table 2: The average values of MAE and R for modern and traditional regression techniques

Method	MAE		R	
	Train dataset	Test dataset	Train dataset	Test dataset
FFNN	**0.022513**	**0.031366**	**0.96599**	**0.933773**
ANFIS	0.024483	0.038636	0.950695	0.924699
MLR	0.027048	0.037098	0.950528	0.923214

8. CONCLUSIONS

The research utilized a comprehensive database primarily focused on Mediterranean Sea basin ferries, with Greece and Italy as the main contributors. The EEXI calculation was done for the created database, and the ships that complied with the IMO requirement were used for further power prediction. The data underwent precise pre-processing, outlier detection, and statistical comparisons between the AI models and traditional technique. Through an investigation, it became evident that AI models have the potential to revolutionize this field. The research compared two different AI architectures, including FFNN, ANFIS and classical multiple linear MLR, throughout two criteria: coefficient of correlation and mean absolute error. Ultimately, the mathematical models developed in this study are versatile and can be implemented in various programming languages or tools. Surprisingly, while FFNN, with its nonlinear nature, displayed the best results in both terms, the best MLR model also demonstrated significant promise especially on the testing data. The optimization of ANFIS parameters and avoiding grid partition which suffers from *the curse of dimensionality* would probably contribute to an enhancement in its performance. The results showed that all three different models have excellent agreement with target values. This research highlights the importance of considering both traditional and AI-based methods when approaching complex engineering problems.

9. APPENDIX

Table 3: Table of neural network parameters (functions representing the output model)

j	$\mathbf{A}_{j1}$	$\mathbf{A}_{j2}$	$\mathbf{A}_{j3}$	$\mathbf{A}_{j4}$	$\mathbf{A}_{j5}$	$\boldsymbol{a}_j$
1	-3.28876	0.33677	4.16012	-4.15641	4.87905	4.65587
2	4.35843	-5.18083	-2.40021	-0.84172	3.76688	-1.0065
3	-3.00178	0.89156	-1.89225	-1.80173	6.1742	0.91508
4	0.43798	0.40144	-3.09167	-8.03634	2.63088	5.63245
5	-2.86924	3.17832	2.2655	1.9607	-5.58485	-7.02272

i	$\mathbf{B}_{i1}$	$\mathbf{B}_{i2}$	$\mathbf{B}_{i3}$	$\mathbf{B}_{i4}$	$\mathbf{B}_{i5}$	$\boldsymbol{b}_i$
1	-5.12563	2.65542	-4.89347	0.52257	3.89146	3.21073
2	3.38835	-1.61511	2.80939	4.96292	-3.85603	-7.36271
3	3.48122	-4.34514	-5.44006	0.34604	3.78631	0.22806
4	2.27801	-1.20839	-6.9587	4.00962	-0.14242	1.51492
5	3.49723	3.07672	-6.75903	0.26026	-3.04861	2.66635
6	-4.65928	5.55562	0.32137	-2.5814	1.913	-3.27717
7	2.7776	4.7746	-0.40907	-3.10186	-5.29917	3.70518

$\mathbf{C}_{11}$	$\mathbf{C}_{12}$	$\mathbf{C}_{13}$	$\mathbf{C}_{i4}$	$\mathbf{C}_{15}$	$\boldsymbol{C}_{16}$	$\mathbf{C}_{17}$	c_1
-3.66054	1.84198	2.80507	-0.21939	-1.18761	1.41906	-4.04158	6.33113
3.38363	2.08991	-4.13246	2.5873	1.80467	-0.25421	1.83586	-6.0888
3.50726	3.50384	1.48631	1.39612	3.32051	-2.4313	-4.1857	-1.96468
3.91898	-4.19942	-0.71853	2.79735	-1.35752	-3.27433	-1.37037	2.49116
3.87391	-0.20698	-4.26104	4.2394	-0.0251	-0.82404	-0.04988	1.51104

k	$\boldsymbol{p}_k$	$\boldsymbol{r}_k$
1	0.1651809	-0.3582328
2	0.1438822	-0.373716
3	1.0647935	-0.0699902
4	0.2819786	-1.1001839
5	1.3832278	-0.2357441

$\mathbf{D}_{11}$	$\mathbf{D}_{12}$	$\mathbf{D}_{13}$	$\mathbf{D}_{i4}$	$\mathbf{D}_{15}$	$\boldsymbol{d}_1$
-0.62147	0.11969	-4.43282	-1.53057	-2.66849	5.60293

L	0.006746
G	0.0049544

Table 4: ANFIS premise and consequent parameters

i=1,2 k=1,…,5	$\boldsymbol{\alpha}_{ik}$	$\boldsymbol{\beta}_{ik}$
A_{11}	0.15934	0.36032
A_{21}	0.95925	0.30352
A_{12}	0.02301	0.07787
A_{22}	0.68993	0.26933
A_{13}	0.10501	0.46661
A_{23}	1.02048	0.26668
A_{14}	0.06216	0.18371
A_{24}	0.93025	0.36031
A_{15}	0.0003	0.28488
A_{25}	0.93952	0.38411

Rule m	$\boldsymbol{q}_{m1}$	$\boldsymbol{q}_{m2}$	$\boldsymbol{q}_{m3}$	$\boldsymbol{q}_{m4}$	$\boldsymbol{q}_{m5}$	$\mathbf{c}_m$
1.	0.07707	0.04148	0.04158	0.06699	0.05042	0.20511
2.	0.02156	0.01398	0.01046	0.02282	0.0207	0.05444
3.	0.02809	0.01803	0.00947	0.02722	0.03794	0.07479
4.	0.0484	0.03253	0.01499	0.06331	0.0594	0.09961
5.	0.01278	0.00813	0.01382	0.01384	0.00731	0.03024
6.	0.00385	0.00626	0.01006	0.00852	0.00973	0.01535
7.	0.01323	0.01009	0.02178	0.01652	0.00851	0.03048
8.	0.00644	0.01262	0.01973	0.01695	0.01986	0.02794
9.	0.03072	0.02597	0.02056	0.03178	0.02421	0.09019
10.	0.02306	0.04766	0.01647	0.04342	0.06457	0.0864
11.	0.01269	0.03132	0.03058	0.03634	0.03864	0.04867
12.	0.04816	0.1492	0.1157	0.1912	0.1964	0.25653
13.	0.00766	0.00863	0.0121	0.01126	0.00611	0.02098
14.	0.00734	0.02059	0.03032	0.02501	0.03309	0.04192
15.	0.03173	0.03157	0.05557	0.04699	0.02235	0.0758
16.	0.03969	0.11222	0.16862	0.14075	0.17978	0.22746
17.	0.02942	0.01236	0.0134	0.02827	0.01632	0.06102
18.	0.0109	0.00505	0.00324	0.0115	0.00905	0.02084
19.	0.0373	0.00998	0.00279	0.03605	0.03747	0.05343
20.	0.05017	0.01924	0.00934	0.05453	0.04051	0.07799
21.	0.00663	0.00322	0.00588	0.00693	0.00301	0.01327
22.	0.00142	0.00083	0.00132	0.00167	0.0011	0.00303
23.	0.00624	0.00386	0.00729	0.0072	0.00377	0.0125
24.	0.00272	0.00155	0.00215	0.00336	0.00229	0.00512
25.	0.00739	0.00565	0.00404	0.00846	0.00517	0.01738
26.	0.00586	0.00616	0.00165	0.00827	0.00862	0.01361
27.	0.00474	0.01281	0.00122	0.0121	0.02058	0.01136
28.	0.02826	0.00739	0.0081	0.03102	0.02427	0.04547
29.	0.00249	0.00205	0.00309	0.00313	0.00113	0.0055
30.	0.00071	0.00103	0.00127	0.00138	0.00139	0.00228
31.	0.01062	0.0093	0.01686	0.01436	0.0041	0.02242
32.	0.00302	0.00414	0.00554	0.00586	0.0052	0.00897

10. ACKNOWLEDGEMENTS

Here shown conclusions are the result of research supported by the Ministry of Science, Technology and Innovations Republic of Serbia under contract 451-03-47/2023-01/200105, subprojects TR-35043 and TR-35004, from 03. 02. 2023. year.

11. REFERENCES

Bayraktar, M., & Sokukcu, M. (2023). Marine vessel energy efficiency performance prediction based on daily reported noon reports, Ships and Offshore Structures, 1-10, doi. https://doi.org/10.1080/17445302.2023.2214490.

Jang J. S. R. (1993) ANFIS: adaptive-network-based fuzzy inference system, IEEE Transactions on Systems, Man, and Cybernetics, 23 (3), 665-685, May-June 1993, doi. https://doi.org/10.1109/21.256541.

Jovanović R. Ž. (2018). Handbook in intelligent control systems, Chapter 4, Multi-Layer Neural Networks, Faculty of Mechanical Engineering, University of Belgrade, Serbia.

Jovanović, R. Ž., Sretenović, A. A., & Živković, B. D. (2015). Ensemble of various neural networks for prediction of heating energy consumption. Energy and Buildings, 94, 189-199, doi. https://doi.org/10.1016/j.enbuild.2015.02.052.

Kalajdžić, M., Vasilev, M., Momčilović, N. (2022). Power reduction considerations for bulk carriers with respect to novel energy efficiency regulations. Brodogradnja: Teorija i praksa brodogradnje i pomorske tehnike, 73(2), 79-92, doi. https://doi.org/10.21278/brod72205.

Lee, J. B., Roh, M. I., & Kim, K. S. (2021). Prediction of ship power based on variation in deep feed-forward neural network, International Journal of Naval Architecture and Ocean Engineering, 13, 641-649, doi. https://doi.org/10.1016/j.ijnaoe.2021.08.001.

MEPC.328(76) Resolution Mepc.328(76) Amendments to the Annex of the Protocol of 1997 to Amend the International Convention for the Prevention of Pollution From Ships, 1973, as Modified by the Protocol of 1978 Relating Thereto https://wwwcdn.imo.org/localresources/en/KnowledgeCentre/IndexofIMOResolutions/MEPCDocuments/MEPC.328(76).pdf

MEPC.333(76) (Adopted On 17 June 2021) Guidelines on the Method of Calculation of the Attained Energy Efficiency Existing Ship Index (EEXI), https://wwwcdn.imo.org/localresources/en/KnowledgeCentre/IndexofIMOResolutions/MEPCDocuments/MEPC.333(76).pdf.

Mijatović L., mentor Kalajdzic M., (2023) Energy efficiency analysis and guidlines for the improvement of Ro-PAX ships, Faculty of Mechanical Engineering, University of Belgrade, Serbia. Master thesis

Mirjalili, S., & Mirjalili, S. (2019). Genetic algorithm. Evolutionary Algorithms and Neural Networks: Theory and Applications, Part of the Studies in Computational Intelligence book series, 780, Springer, Cham. 43-55, doi. https://doi.org/10.1007/978-3-319-93025-1_4.

Öztürk, O. B., & Başar, E. (2022). Multiple linear regression analysis and artificial neural networks based decision support system for energy efficiency in shipping, Ocean Engineering, 243, 110209, doi. https://doi.org/10.1016/j.oceaneng.2021.110209.

Ozsari, I. (2023). Predicting main engine power and emissions for container, cargo, and tanker ships with artificial neural network analysis, Brodogradnja: Teorija i praksa brodogradnje i pomorske tehnike, 74(2), 77-94, doi. https://doi.org/10.21278/brod74204.

Parkes, A. I., Sobey, A. J., & Hudson, D. A. (2018). Physics-based shaft power prediction for large merchant ships using neural networks, Ocean Engineering, 166, 92-104, doi. https://doi.org/10.1016/j.oceaneng.2018.07.060.

Radojčić, D., Kalajdžić, M., Simić, A. (2019). Power Prediction Modeling of Conventional High-Speed Craft, 1st ed. 2019 Edition, Springer International Publishing. ISBN 978-3-030-30606-9.

Radojčić, D., Zgradić, A., Kalajdžić, M., & Simić, A. (2014). Resistance prediction for hard chine hulls in the pre-planing regime, Polish Maritime Research, 21(2), 9-26, doi. https://doi.org/10.2478/pomr-2014-0014.

Vesović, M., Jovanović, R. (2022). Adaptive neuro fuzzy Inference systems in identification, modeling and control: The state-of-the-art, Tehnika, 77(4), 439-446, doi. https://doi.org/10.5937/tehnika2204439V.

Vesović, M., Jovanović, R. (2023). Heat Flow Process Identification Using ANFIS-GA Model. In Sinteza 2023-International Scientific Conference on Information Technology and Data Related Research, Belgrade, Singidunum University, Serbia, 2023, pp. 44-51 (pp. 44-51). Belgrade: Singidunum University. doi. https://doi.org/10.15308/Sinteza-2023-44-51.

https://www.shippax.com/ (last accessed 05. 07. 2023).